XXI IMEKO World Congress "Measurement in Research and Industry"
August 30 – September 4, 2015, Prague, Czech Republic

ESTIMATION OF PEIODIC SIGNAL PARAMETERS BY SIGNAL AND ZERO PADDING

Dušan Agrež [1], *Damir Ilić* [2], *Janko Drnovšek* [1]

[1] University of Ljubljana, Faculty of Electrical Engineering, Ljubljana, Slovenia, e-mail: dusan.agrez@fe.uni-lj
[2] University of Zagreb, Faculty of Electrical Engineering and Computing, Zagreb, Croatia, e-mail: Damir.Ilic@fer.hr

Abstract – In paper, a frequency domain algorithm for estimation of the sine signal parameters in the case of signal sampling by averaging in the aperture time is presented. Prior to estimations in the frequency domain the sampled signal is padded with the signal average values in the aperture times and zeroes outside. We can increase padding points and with this nearing the errors to the level as with estimations of the signal without average sampling.

Keywords: sampling dynamics, signal padding, zero padding, interpolated DFT.

1. INTRODUCTION

Parameter's estimations of periodic signals mostly base on sampling and acquiring digital values of samples by analog-to-digital converters. In this procedure values of sampling points are results of averaging in the aperture time – measurement time. This averaging (or integration) gives reduction of noise but causes systematic errors in estimations of the signal parameters [1], [2]. In this paper, algorithms for estimations of amplitude and frequency by signal and zero padding first and then interpolation in the frequency domain are presented.

Sampling process can be modeled with four signals and their frequency spectra in time and frequency domains: measured signal $g(t) \overset{\mathrm{F}}{\longleftrightarrow} G(f)$, impulse response of the sampling channel $h(t) \overset{\mathrm{F}}{\longleftrightarrow} H(f)$ (Fig.1), sampling function $s(t) \overset{\mathrm{F}}{\longleftrightarrow} S(f)$ (Fig.2), and the window function of the measurement interval $w(t) \overset{\mathrm{F}}{\longleftrightarrow} W(f)$ (Fig.3).

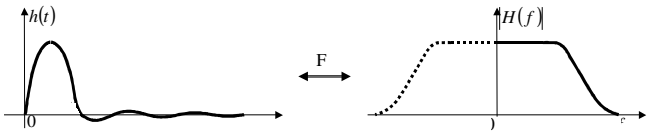

Fig. 1 Impulse response of the sampling channel

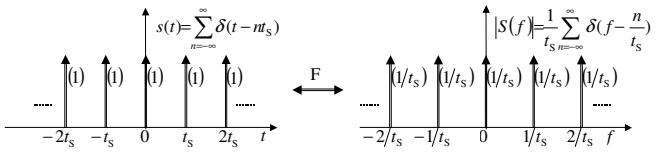

Fig. 2 Sampling function in the time and frequency domain

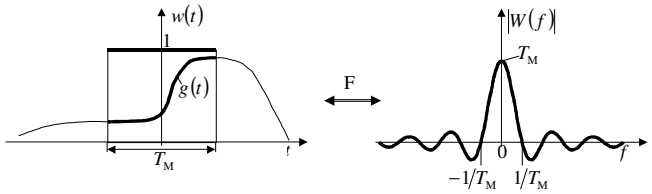

Fig. 3 Window function of the measurement interval

Considering that equivalent of multiplication in the time domain is convolution in the frequency domain $\times \equiv g_1(t) \times g_2(t) \overset{\mathrm{F}}{\longleftrightarrow} \otimes \equiv \int_{-\infty}^{\infty} G_1(\nu) G_2(f-\nu)\mathrm{d}\nu$ and vice versa $\otimes \equiv \int_{-\infty}^{\infty} g_1(\tau) g_2(t-\tau)\mathrm{d}\tau \overset{\mathrm{F}}{\longleftrightarrow} \times \equiv G_1(f) \times G_2(f)$ [3] the sampling procedure can be modeled as follows (Fig. 4):

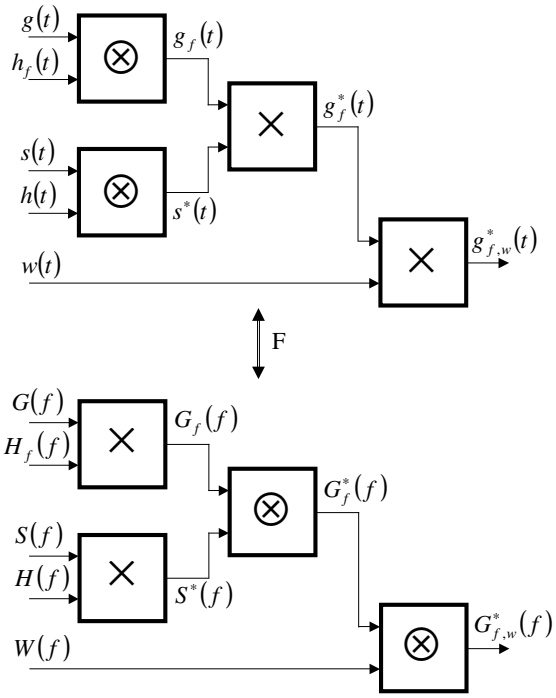

Fig. 4 Procedure of sampling in the time and frequency domains

It is evident that with modification of sampling pulses $h(t) \overset{\mathrm{F}}{\longleftrightarrow} H(f)$ we changing spectrum of the sampled signal (Fig. 5).

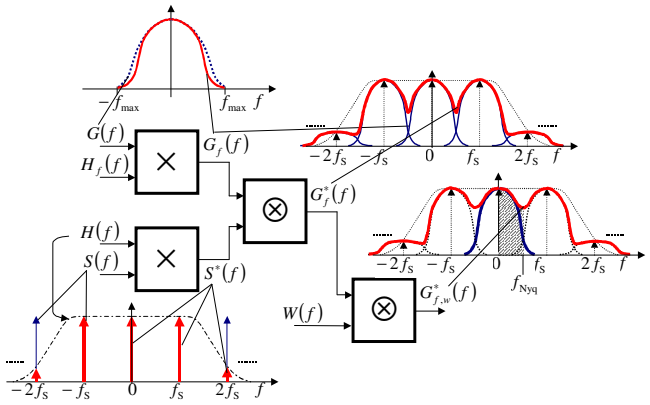

Fig. 5 Spectra of signals in the sampling process

2. ESTIMATION OF PARAMETERS

Sampling by frequency $f_S = 1/t_S$ of the periodic band limited analog signal $g(t)$ composed of M components can be expressed as $w(nt_S)\cdot\sum_{m=0}^{M-1} A_m \sin(2\pi f_m nt_S + \varphi_m)$ with f_m, A_m, and φ_m as frequency, amplitude, and phase of particular component, respectively. In estimation procedure one has to take into account that values of samples (Fig. 6d) are representatives in the aperture time t_{ap} or typically average values of the signal in the aperture integration interval (Fig. 6c). For demonstration of sampling in Fig. 6 three periods of the one component sine signal are presented with duty cycle of sampling $D = t_{ap}/t_S = 0.4$ and with sampling ratio of $r = f_S/f_m = T_m/t_S = 1.6$.

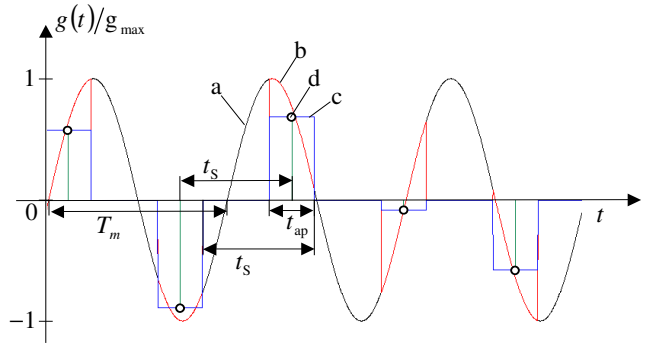

Fig. 6 Signals of sampling by averaging in the aperture time: a – original signal, b – truncated signal in the aperture intervals, c – average values signal in the aperture integration interval, d – average value representatives of the sampled signal in the aperture integration interval

With sampling representatives – average values – we lose some information of the signal and especially in the cases where the aperture time is so long that signal change significantly in this interval and where the sampling Nyquist condition is not fulfilled. One possibility to overcome these problems is to add zeroes (known as zero-padding technique [4]) and average values in the aperture times with the duty ratio $D = t_{ap}/t_S$, which is defined by the ratio of the aperture time t_{ap} and the sampling interval t_S (Fig. 6c). Aperture time is positioned symmetrically around knowing sampling instants.

With increased number of samples is possible to detect signals below Nyquist condition (Fig. 7: The whole acquired signal contain around 50 cycles of sinusoid $\theta_m = f_m/\Delta f = f_m \cdot Nt_S \doteq 50$ on $N = 20$k points). An undersampled sine wave still appears as a sampled sine wave but at a lower frequency $f' = |kf_S - f_m|$ ($k = 1, 2, ...$) or expressed by the relative frequency $\theta' = |k\theta_S - \theta_m|$.

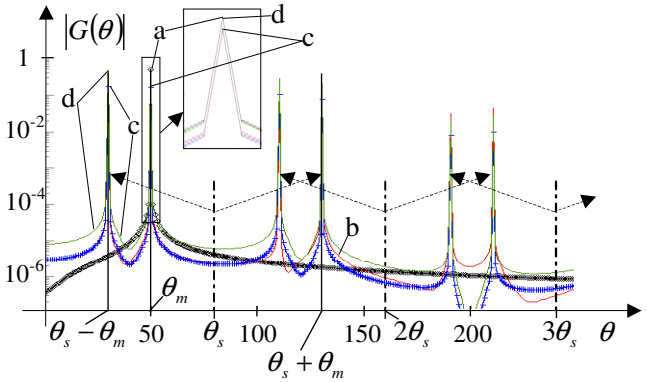

Fig. 7 Spectra of signals from Fig. 6: a – original signal, b – truncated signal in the aperture intervals, c – average values signal in the aperture integration interval, d – average values signal in the aperture integration interval with *sinc* correction.

To estimate parameters of the time-dependent signals containing any periodicity, it is preferable to use a transformation of the signal in the frequency domain. The discrete Fourier transformation of the windowed signal $w(k)\cdot g(k)$ on N sampled points at the spectral line i is given by:

$$G(i) = -\frac{\mathrm{j}}{2}\sum_{m=0}^{M} A_m\left(W(i-\theta_m)\mathrm{e}^{\mathrm{j}\varphi_m} - W(i+\theta_m)\mathrm{e}^{-\mathrm{j}\varphi_m}\right) \qquad (1)$$

where $\theta_m = f_m/\Delta f = i_m + \delta_m$ is the component frequency related to base frequency resolution $\Delta f = 1/T_M = 1/Nt_S$ and consists of an integer part and the non-coherent sampling displacement term $-0.5 \le \delta_m < 0.5$.

A finite time of measurement is a source of dynamic errors, which are shown as leakage parts of the measurement window spectrum convolved on the spectrum of the measured-sampled signal (Fig. 7). Tones of the sampled signal do not generally coincide with the basis set of the periodic components of the discrete Fourier transformation (DFT), which is the most well known non-parametric method for frequency decomposition of signals [5].

The long-range leakage contributions can be reduced in more ways: by increasing the measurement time $\Delta f_{\downarrow} = 1/T_{meas\uparrow}$, by using windows with a faster reduction of the side lobes (like the Rife-Vincent windows class I - RV1, etc.), or by using the multi-point interpolated DFT algorithms.

Parameters of the measurement component can be estimated by means of the interpolation [6]. From the comparative study [7] it can be concluded that the key for

estimating the three basic parameters is in determining the position of the measurement component $\delta_m = \theta_m - i_m$ between DFT coefficients $G(i_m)$ and $G(i_m+1)$ surrounding the component m. In estimations, the well-known expressions for the three-point estimations for frequency (2) and amplitude (3) were used. The three-point DFT interpolation gives the optimum results: it is symmetric around the local peak amplitude DFT coefficient; equally suppress leakages coming from both sides; the minimal error curves are equal as with one-, five- and multi-point interpolations except the order P of windows have to be changed using RV1 windows [6].

$$ {}_3\delta_m \doteq (P+1)\cdot \frac{|G(i_m+1)|-|G(i_m-1)|}{|G(i_m-1)|+2|G(i_m)|+|G(i_m+1)|} \qquad (2) $$

$$ {}_3A_m \doteq 2\left|\frac{2^{2P}}{(2P+2)!}\cdot\frac{\pi\delta_m}{\sin(\pi\delta_m)}\cdot\prod_{l=1}^{P+1}\left(l^2-\delta_m^2\right)\right|\cdot \cdot\left(|G(i_m-1)|+2|G(i_m)|+|G(i_m+1)|\right) \qquad (3) $$

3. EVALUATION OF THE ESTIMATIONS

We can estimate parameters of particular component (true or apparent on Fig. 7) by the three-point interpolations since we need only local largest DFT coefficients. The estimation errors were compared for the frequency (2) and amplitude (3) estimations using the Hann window ($P=1$). The absolute errors of the frequency estimation $|E(\theta)| = |\theta_{\text{est.}} - \theta_{\text{true}}|$ and the absolute relative errors of the amplitude estimation $|e(A)| = |A_{\text{est.}}/A_{\text{true}} - 1|$ are checked for one sine component in the signal with a double scan, varying specific parameter and the phase of the signal at particular relative frequency because the long-range leakages are frequency- and phase-dependent (Figs. 8-17: $A_m = 1$, and $-\pi/2 \le \varphi \le \pi/2$, $\Delta\varphi = \pi/18$).

First, the sampling ratio $r = f_S/f_m$ was changed to find intervals where the interpolation algorithm can be used (Figs. 8 and 13). The absolute maximum values of errors (from 19 iterations) at a given sampling ratio are compared using the duty ratio of $D = t_{ap}/t_S = 0.4$.

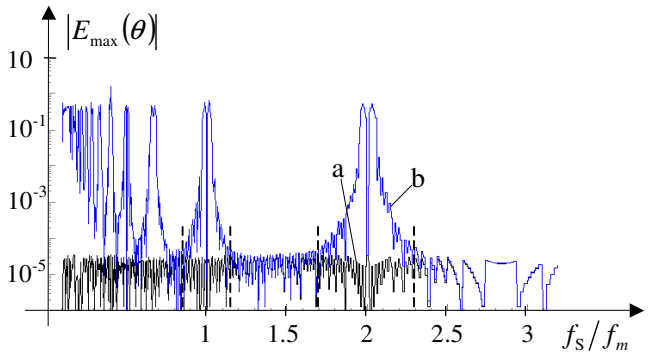

Fig. 8 Absolute maximum values of errors of the frequency estimation in relation to the sampling ratio: a – original signal, b – average values signal; $N = 20\text{k}$, $\theta \doteq 50$, $N_p = 400$

In Fig. 8, we can see that it is possible to estimate frequency of one component even better than if we have complete signal also when the sampling ratio $r = f_S/f_m$ is in interval between 1 and 2 (sampling condition is not fulfilled). The vicinity around integer values 1 and 2 where we can't estimate parameters as in the case of original signal depends on the number of signal cycles in the whole measurement interval T_M.

Largest value θ gives better frequency resolution and borders come closer to integer values 1 and 2 (Figs. 8, 9, and 10). If we have enough sampling points in one period ($N_p = 400$ points are used in simulations from analysis in Figs. 16 and 17) the width of the error estimation main-lobe around integer values the sampling ratio 1 and 2 depends on the position of the investigated component θ and interspacing between neighboring components. If we have $\theta = 50$ cycles in the measurement interval (Fig. 8) we get basic bin resolution $1/50$ and this resolution gives error main-lobe borders $0.85 < r < 1.15$ and $1.7 < r < 2.3$ around integers where the frequency estimation errors increase due to leakage influence on the investigated component θ_m from its replicas $k\theta_S - \theta_m$, $k = 1, 2$ (Fig. 7). It can be also noticed that there are error peaks which number increase below $r = 2/3$ due to replicas $|k\theta_S - \theta_m|$ with higher values of $k = 3, 4, ..$ (Fig. 10).

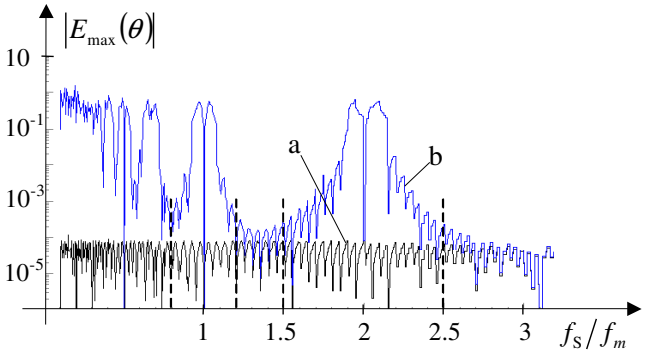

Fig. 9 Absolute maximum values of errors of the frequency estimation in relation to the sampling ratio: a – original signal, b – average values signal; $N = 8\text{k}$, $\theta \doteq 20$, $N_p = 400$

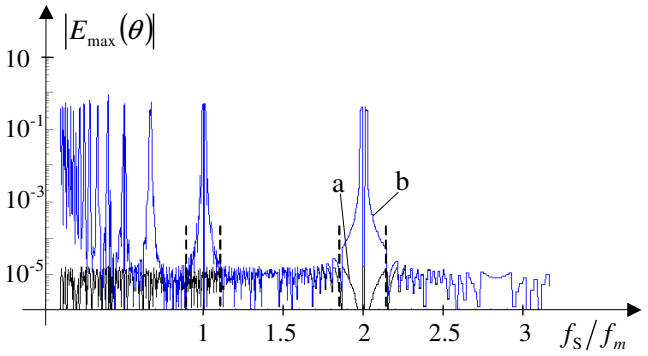

Fig. 10 Absolute maximum values of errors of the frequency estimation in relation to the sampling ratio: a – original signal, b – average values signal; $N = 40\text{k}$, $\theta \doteq 100$, $N_p = 400$

Decreasing bin resolution to $1/20$ increases unusable intervals to $0.8 < r < 1.2$ and $1.5 < r < 2.5$ (Fig. 9). Going in opposite direction by increasing bin resolution to $1/100$ (Fig. 10) reduces unusable intervals to $0.9 < r < 1.1$ and $1.85 < r < 2.15$, and the frequency can be accurately estimated also in the interval of sampling ratio $1.1 < f_S/f_m < 1.85$ what is below sampling condition.

In the case of the amplitude estimation (Figs. 11, 12, and 13) we need to correct the estimated amplitude or the complete amplitude DFT spectrum (Fig. 7d) by well-known *sinc* correction $k_{\text{corr-sinc}} = (\pi \cdot t_{\text{ap}}/t_{\text{p}})/\sin(\pi \cdot t_{\text{ap}}/t_{\text{p}})$ [1].

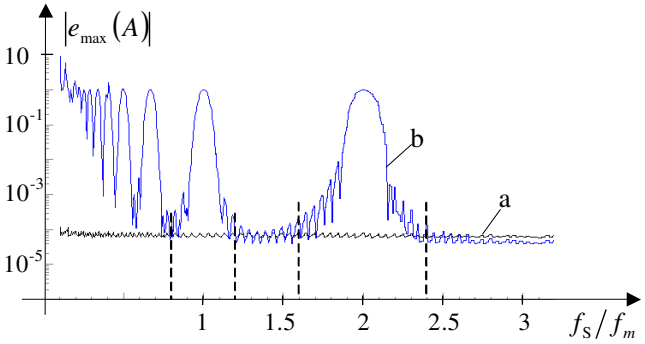

Fig. 11 Absolute maximum values of relative errors of the amplitude estimation in relation to the sampling ratio: a – original signal, b – average values signal; $N = 8\text{k}$, $\theta \doteq 20$, $N_{\text{p}} = 400$

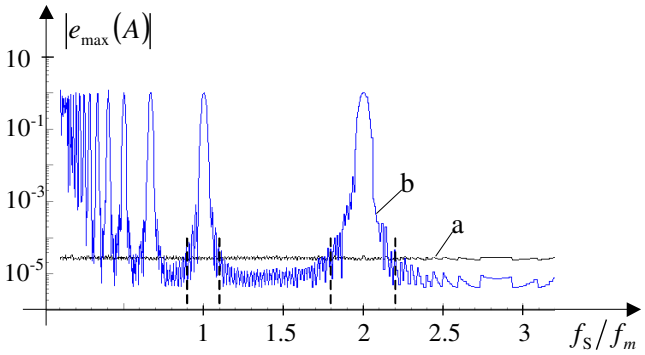

Fig. 12 Absolute maximum values of relative errors of the amplitude estimation in relation to the sampling ratio: a – original signal, b – average values signal; $N = 20\text{k}$, $\theta \doteq 50$, $N_{\text{p}} = 400$

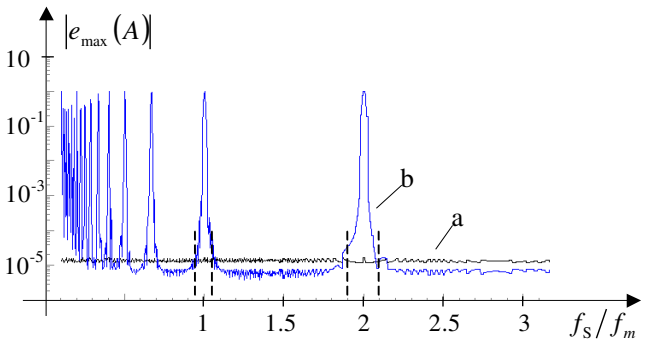

Fig. 13 Absolute maximum values of relative errors of the amplitude estimation in relation to the sampling ratio: a – original signal, b – average values signal; $N = 40\text{k}$, $\theta \doteq 100$, $N_{\text{p}} = 400$

We can see the same behaviors of the errors in the case of amplitude estimation as with the frequency estimation (Figs. 11, 12, and 13). Bin resolution of $1/20$ gives unusable intervals $0.8 < r < 1.2$ and $1.6 < r < 2.4$ (Fig. 11), resolution of $1/50$ reduce unusable intervals $0.9 < r < 1.1$ and $1.8 < r < 2.2$ (Fig. 12), and resolution of $1/100$ further reduce unusable intervals to $0.95 < r < 1.05$ and $1.9 < r < 2.1$ (Fig. 13).

If we change the duty ratio $D = t_{\text{ap}}/t_{\text{S}}$ in the sampling interval (changing the aperture time at fix sampling frequency) the estimation errors do not change very much in comparison to estimations on original signal if we correct the estimation by *sinc* correction. In Figs. 14 and 15 the duty ratio was changed almost in the whole possible interval $D = 0.001 \div 0.998$ at $r = f_S/f_m = 1.6$ with $N_{\text{P}} = 400$ samples in one period (other parameters were the same as in Fig. 6)

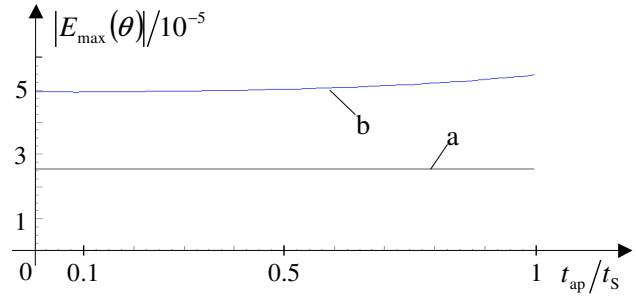

Fig. 14 Absolute maximum values of errors of the frequency estimation in relation to the duty ratio: a – original signal, b – average values signal in the aperture interval

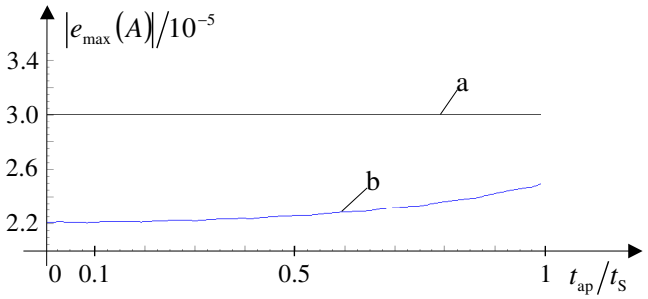

Fig. 15 Absolute maximum values of relative errors of the amplitude estimation in relation to the duty ratio: a – original signal, b – average values signal in the aperture integration interval with *sinc* correction

Estimations also much depend on the number of sampling points in the period N_P and in the whole measurement interval. Padding with more points (average signal values and zero values) will improve estimations since interpolation equations (2) and (3) are derived for large values of points $N >> 1$ [6]. In Figs. 16 and 17 the number of sampling points in the period N_P was changed from $N_{\text{P}} = 10$ to more than $N_{\text{P}} = 512$ (other parameters were the same as in Fig. 6). We can see that frequency estimation do not differ significantly if we have reduced

information of the signal (Fig. 16: curves a and b) and both errors of estimations degrease with increasing number of points.

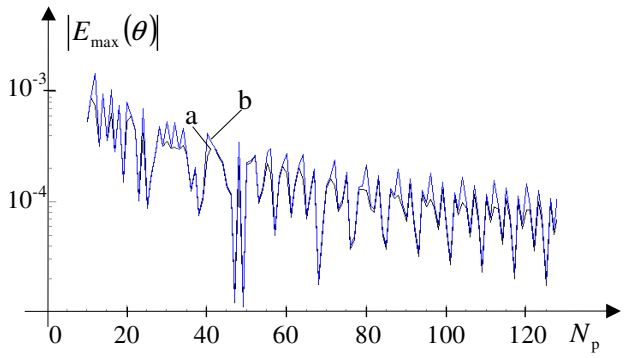

Fig. 16 Absolute maximum values of errors of the frequency estimation in relation to the number of sampling points in the period: a – original signal, b – average values signal in the aperture interval.

Amplitude estimations much more depend on the number of points (Fig. 17) but after having more than $N_P = 128$ sampling points in the period the estimation errors drop on the level as with estimation on the original signal without averaging in the aperture time.

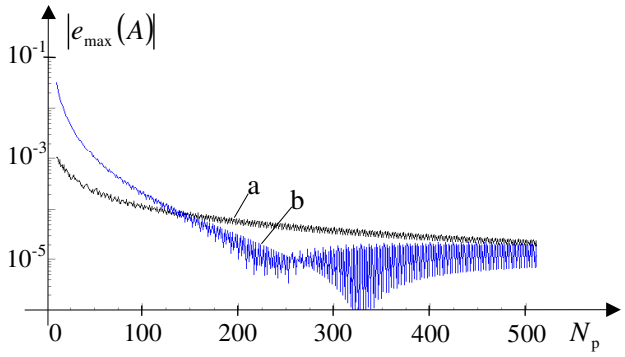

Fig. 17 Absolute maximum values of relative errors of the amplitude estimation in relation to the number of sampling points in the period: a – original signal, b – average values signal in the aperture integration interval with *sinc* correction

The price for the effective leakage reduction is in the increase of the estimation uncertainties related to the unbiased Cramér-Rao bounds [8] fixed by the signal-to-noise-ratio for a particular component $SNR_m = A_m^2/(2\sigma_t^2)$ corrupted by a white noise with standard uncertainty σ_t [9]. In Figs. 18 and 19, there are standard uncertainties of the frequency and amplitude estimations related to the CR bounds, respectively.

$$\sigma_\theta \geq \frac{\sqrt{3}}{\pi}\frac{1}{\sqrt{SNR}}\frac{1}{\sqrt{N}} = \sigma_{CRB,\theta} \quad (4)$$

$$\sigma_A \geq \frac{1}{\sqrt{SNR}}\frac{1}{\sqrt{N}} = \sigma_{CRB,A} \quad (5)$$

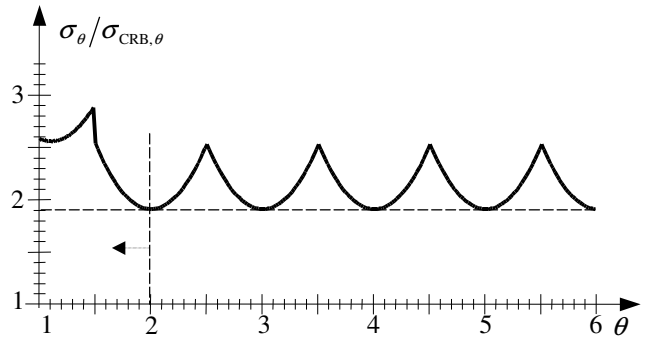

Fig. 18 Standard uncertainty of the three-point displacement estimation (2) related to the CR bound (4)

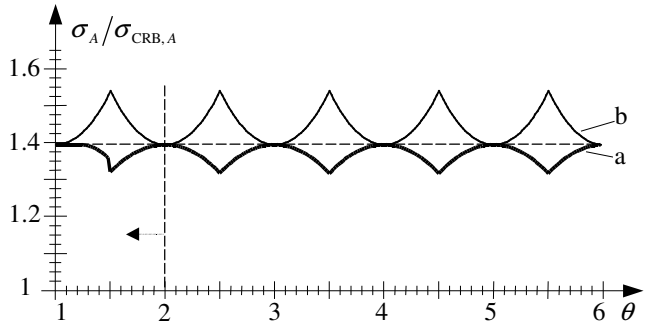

Fig. 19 Standard uncertainty of the amplitude three-point estimation (3) related to the CRB (5) (a: θ is estimated, b: θ is known

Moving away from integers of the relative frequency, what is the case when the sampling ratio is below 2, the standard uncertainties increase in relation to the minimal attainable values (Fig. 18 for frequency estimation and Fig. 19 for amplitude estimation) but changes can be neglected. In the case of amplitude estimation the standard deviation even decreases if the frequency θ is estimated first.

4. CONCLUSIONS

In the proposed paper, algorithms for estimation of amplitude and frequency by signal and zero padding first and then interpolation in the frequency domain are presented. Signal and zero padding enable estimations of the parameters of the particular component by interpolated DFT. In many cases a number of sampling points is limited but in algorithms on computer we can increase padding points and with this nearing the errors to the level as with estimation on the original signal without averaging in the aperture time.

REFERENCES

[1] R. L. Swerlein, “A 10 ppm accurate digitalAC measurement algorithm,” in *Proc. NCSL Workshop Symp.*, pp. 17–36. 1991.

[2] G. A. Kyriazis, "Extension of Swerlein’s Algorithm for AC Voltage Measurement in the Frequency Domain ", IEEE Trans. Instrum. Meas., vol. 52, no. 2, pp. 367-370, April 2003.

[3] W. McC. Siebert: Circuits, Signals and Systems, The MIT Press, McGraw-Hill, Cambridge, New York, ..., pp. 497-502, 1986.

[4] G. Leus, M. Moonen, "Semi-blind channel estimation for block transmissions with non-zero padding", *Records of Conference on Signals, Systems and Computers*, pp. 762-766, Nov 2001.

[5] F. J. Harris: " On the use of windows for harmonic analysis with the discrete Fourier transform", Proc. IEEE, vol. 66, no. 1, pp. 51-83, January 1978.

[6] J. Štremfelj and D. Agrež, "'Nonparametric estimation of power quantities in the frequency domain using Rife-Vincent windows," *IEEE Trans. Instrum. Meas.*, vol. 62, no. 8, pp. 2171-2184, Aug. 2013.

[7] J. Schoukens, R. Pintelon, and H. Van hamme: "The interpolated fast Fourier transform: A comparative study", IEEE Trans. Instrum. Meas., vol. 41, no. 2, pp. 226-232, April 1992.

[8] A. Moschitta and P. Carbone, "Cramer-Rao lower bound for parametric estimation of quantized sinewaves," in *Proc. IEEE IMTC/2004*, Como, Italy, May 2004, pp. 1724–1729.

[9] Widrow B, Kollar I, 'Quantization Noise', Cambridge Univ. Press, 2008.